Polygons and Adhesion Plaques and the Disassembly and Assembly of Myofibrils in Cardiac Myocytes

Zhongxiang Lin,*‡ Sybil Holtzer,* Thomas Schultheiss,* John Murray,* Tomoh Masaki,§ Donald A. Fischman,‖ and Howard Holtzer*

*Department of Anatomy, School of Medicine, University of Pennsylvania, Philadelphia, Pennsylvania 19104; ‡Department of Cell Biology, Beijing Institute for Cancer Research, Beijing, China; §Institute of Basic Medical Sciences, University of Tsukaba, Tsukaba, Japan; and ‖Department of Cell Biology and Anatomy, Cornell University Medical College, New York 10021

Abstract. Successive stages in the disassembly of myofibrils and the subsequent assembly of new myofibrils have been studied in cultures of dissociated chick cardiac myocytes. The myofibrils in trypsinized and dispersed myocytes are sequentially disassembled during the first 3 d of culture. They split longitudinally and then assemble into transitory polygons. Multiples of single sarcomeres, the cardiac polygons, are analogous to the transitory polygonal configurations assumed by stress fibers in spreading fibroblasts. They differ from their counterparts in fibroblasts in that they consist of muscle α-actinin vertices and muscle myosin heavy chain struts, rather than of the nonmuscle contractile protein isoforms of stress fiber polygons. EM sections reveal the vertices and struts in cardiac polygons to be typical Z and A bands. Most cardiac polygons are eliminated by day 5 of culture. Concurrent with the disassembly and elimination of the original myofibrils new myofibrils are rapidly assembled elsewhere in the same myocyte. Without exception both distal tips of each nascent myofibril terminate in

adhesion plaques. The morphology and composition of the adhesion plaques capping each end of each myofibril are similar to those of the termini of stress fibers in fibroblasts. However, whereas the adhesion complexes involving stress fibers in fibroblasts consist of vinculin/nonmuscle α-actinin/β- and γ-actins, the analogous structures in myocytes involving myofibrils consist of vinculin/muscle α-actinin/α-actin. The addition of 1.7–2.0 μm sarcomeres to the distal tips of an elongating myofibril, irrespective of whether the myofibril consists of 1, 10, or several hundred tandem sarcomeres, occurs while the myofibril appears to remain linked to its respective adhesion plaques. The adhesion plaques in vitro are the equivalent of the in vivo intercalated discs, both in terms of their molecular composition and with respect to their functioning as initiating sites for the assembly of new sarcomeres. How 1.7–2.0 μm nascent sarcomeres can be added distally during elongation while the tips of the myofibrils remain inserted into submembranous adhesion plaques is unknown.

O VER the past decade much new information has accumulated regarding the multiple genes that encode the myofibrillar proteins in skeletal and cardiac muscle cells. During this same period less attention has been directed to how, after their synthesis, the various myofibrillar isoforms rapidly assemble into invariant, tandem sarcomeres (references 13, 42, 46).

Work based on cultured skeletal postmitotic mononucleated myoblasts and myotubes has suggested that subsarcolemmal, stress fiber–like structures (SFLS)[1] serve as initiation or nucleation loci for the assembly of individual myofibrils (2, 12, 34). These submembranous bundles of long filaments stain in a continuous pattern with phalloidin, as well as with antibodies to β- and γ-actin, but in a discontinuous fashion with antibodies to nonmuscle myosin heavy chain

(MHC) and nonmuscle α-actinin. SFLS progressively transform into nascent nonstriated myofibrils by the replacement of β- and γ-actin microfilaments with 1.0-μm-long α-actin thin filaments and by the replacement of nonmuscle myosin filaments with muscle-specific 1.6-μm-long thick filaments (2). EM studies of skeletal and cardiac muscle cells show SFLS as consisting of rows of irregularly shaped, discontinuous dense bodies interconnected by numerous thin filaments (2, 27, 30, 33). The transition from SFLS to nonstriated myofibrils is gradual, both temporally and spatially. In both the fluorescence and electron microscopes it is difficult to determine where, in an immature myogenic cell (a) the nonmuscle α-actinin dense bodies with their inserted β- and γ-actin thin filaments end and where (b) the muscle-specific α-actinin dense bodies of the early assembling Z bands with their inserted and polarized α-actin thin filaments begin. As more and more myofibrillar 1.6-μm-long thick filaments and 1.0-μm-long thin filaments with associated Z bands accumu-

---

1. *Abbreviations used in this paper:* anti-LMM, muscle-specific light meromyosin; MHC, myosin heavy chain; SFLS, stress fiber–like structures.

late and intermingle with the SFLS, the latter cease to stain with antibodies to nonmuscle MHC, the nonmuscle actins, and nonmuscle α-actinin and begin to bind antibodies to muscle MHC, α-actin, and muscle α-actinin. At this stage of maturation emerging myofibrils consist of longitudinally staggered 1.6-μm-long thick filaments intermixed with irregularly distributed I–Z–I complexes. These nascent non-striated myofibrils gradually transform into nascent striated myofibrils with a minimal sarcomeric periodicity of 1.7–2.0 μm (2, 12, 22, 23, 25, 28). It is important to learn more of (a) how longitudinally staggered 1.6-μm-long thick filaments secondarily interdigitate with longitudinally staggered I–Z–I complexes to form typical sarcomeres, and (b) how myocytes concurrently regulate the synthesis and assembly of nonmuscle and muscle-specific contractile proteins into SFLS and striated myofibrils, respectively (1, 11, 12, 24, 34, 48).

Cultures of normal chick skeletal myogenic cells have been useful for studying many aspects of myogenesis (1, 11, 15, 17, 24, 39). Owing, however, to their overall morphology (narrow and thick) these cells have limitations with regard to detailed observations using labeled antibodies. For this purpose cultured chick embryo cardiac myocytes have several advantages. Between days 3 and 7 of culture cardiac myocytes increase their content of muscle-specific MHC and α-actin 8–10-fold and there is a corresponding increase in the number and length of individual myofibrils per cell (3, 7, 8, 9, 14). Cultured myocytes which flatten to form sizeable cytoplasmic regions well-removed from the centrally located nucleus may be <0.5 μm in thickness. As a consequence, cardiac cells are more favorable than skeletal cells for detailed observations of the spatial relationships among myofibrillar proteins before, and during, their assembly into myofibrils.

In this study we follow in cultured cardiac myocytes first the rearrangement and loss of those myofibrils that had been assembled in vivo before plating, and then we follow the earliest stages in the assembly of new myofibrils that form in vitro. Evidence for the close relationship between the contractile protein isoforms in stress fibers in fibroblasts and those in myofibrils is provided by finding that: (a) flattening myocytes form short-lived polygonal networks similar to those formed by stress fibers in nonmuscle cells (31, 32, 42, 43); (b) the vertices and struts in the fibroblast polygons are assembled from nonmuscle contractile protein isoforms, whereas those in cardiac myocytes are assembled from muscle specific isoforms; (c) both the termini of stress fibers in nonmuscle cells (5, 6, 18, 19, 49, 50) and the termini of elongating cardiac myofibrils insert into talin/vinculin adhesion plaques, the former by way of nonmuscle α-actinin and β- and γ-actins, the latter by way of muscle α-actinin and α-actin. The last finding opens the possibility that the adhesion plaques capping the distal tips of nascent elongating myofibrils in myocytes play a role in nucleating and/or stabilizing myofibrils analogous to their role in nucleating and/or stabilizing stress fibers in nonmuscle cells.

Materials and Methods

Cell Culture

Chick cardiac cultures were prepared from 5- to 7-d embryos using a modification of previously described procedures (12). Tissue fragments were incubated in 10 ml of trypsin solution (0.05% trypsin; Gibco Laboratories, Grand Island, NY; in Ca⁺⁺- and Mg⁺⁺- free balanced salt solution) for 10 min at 37°C in 5% CO_2 humidified incubator. The supernatant from this first incubation, presumably containing dissociated cells damaged during tissue processing, was removed and discarded, with care taken to avoid removing any tissue fragments. Fresh trypsin solution (3.5 ml) was added and the tissue incubated for 8 min. The supernatant containing dispersed cardiac cells was removed and placed into a 25-ml vol of chilled (4°C) nutrient medium (5% FCS, 50 U/ml penicillin, 50 μg/ml streptomycin, and 2 mM glutamine in MEM with Earle's salts; Gibco Laboratories). The remaining tissue fragments were incubated in 3.5 ml of fresh trypsin solution as above and the dispersed cells harvested for an additional three to five times. After removal of the supernatant after the final trypsinization, the remaining tissue fragments were gently dissociated in 3.5 ml of growth medium by repeated pipetting, combined with the previously harvested cells, and centrifuged for 10 min. The cell suspension was filtered through lens tissue to remove large clumps of cells. The approximate yield was 0.5–2.0 million cells per heart depending on the age of the embryo.

Cells were grown on glass coverslips at an initial density of 2.0–3.5 × 10 cells/35-mm tissue culture dish in a humidified 5% CO_2 incubator. The day after plating, nutrient medium was replaced with glutamine-free medium (5% FCS 50 U/ml penicillin, 50 μg/ml streptomycin in MEM). Elimination of glutamine from the medium has been shown to facilitate the culture of cardiac myocytes by greatly reducing the proliferation of cardiac fibroblasts (12). Glutamine-free medium was replaced one to three times weekly. Using the above technique, beating cardiac myocytes have been maintained for more than 4 wk in culture. Most observations were made on day 2–7 cultures.

Antibodies

The properties of the polyalonal antibodies to smooth muscle desmin, the brain MHC, the muscle-specific light meromyosin (anti-LMM), and the mouse monoclonal antibody to muscle-specific MHC have been described (2, 4, 15, 34). The brain anti-MHC was a gift from Dr. V. Nachmias whereas the mAb to MHC was a gift from Dr. F. Pepe, both from the University of Pennsylvania. Anti-talin rabbit antiserum, an affinity-purified antibody, was a gift of Dr. K. Burridge, University of North Carolina. The antibody against chicken gizzard vinculin, VIN-11-5, a mouse monoclonal antibody (ICN Immunobiological, Lisle, IL), reacts specifically with vinculin on immunoblots and stains adhesion plaques of cultured cells briefly fixed in formalin. A mouse monoclonal antibody, mAb B4, was a gift of Dr. J. L. Lessard, University of Cincinnati. This antibody was used to detect the presence or absence of α-actin. mAb B4 binds to all four known muscle-specific actins (α-skeletal, α-cardiac, α-vascular, γ-enteric) in immunoblot experiments and in immunofluorescence microscopy using methanol-fixed cells (33). Four kinds of antibodies were used to differentiate nonmuscle from muscle-specific α-actinin in cultured myogenic cells. Rabbit antibodies against smooth muscle α-actinin were a gift of Dr. S. Craig, Johns Hopkins University (Baltimore, MD), and guinea pig antibodies against smooth muscle α-actinin were a gift of Dr. Hans-Peter Kapprell, University of Cologne. Both of these α-actinin antibodies stain the dense bodies of stress fibers in nonmuscle cells in a punctate fashion, as well as lightly staining Z bands and their precursor structures in myogenic cells. In contrast, a mouse monoclonal antibody, mAb CP4-10, and an affinity-purified rabbit antiserum against muscle α-actinin do not stain dense bodies in stress fibers of nonmuscle cells but stain Z bands and their precursor structures intensely in both cardiac and skeletal myogenic cells (15, 34, 35). The antibodies that stain dense bodies in stress fibers in nonmuscle cells as well as Z bands in muscle cells will be referred to as "nonmuscle anti-α-actinin;" those that stain only Z bands and their precursor structures in myogenic cells will be referred to as "muscle anti-α-actinin."

Immunofluorescence and EM Microscopy

Cells were processed for immunofluorescence microscopy as follows: Cultures were rinsed with PBS and fixed for 3 min in 2% formaldehyde (freshly prepared from paraformaldehyde) in PBS. The cells were then permeabilized and soluble proteins extracted, using 0.5% Triton X-100 in PBS. This PBS–Triton solution was also used for all subsequent antibody-washing steps. For staining with mAb B4, cells were fixed for 5 min in cold (−20°C) methanol. Various sequences of antibody and reagent incubations were used in the double-label staining preparations. The binding sites of antibodies to MHC, α-actin, α-actinin, talin, and vinculin were visualized by indirect immunofluorescence microscopy whereas FITC-labeled rabbit anti-LMM
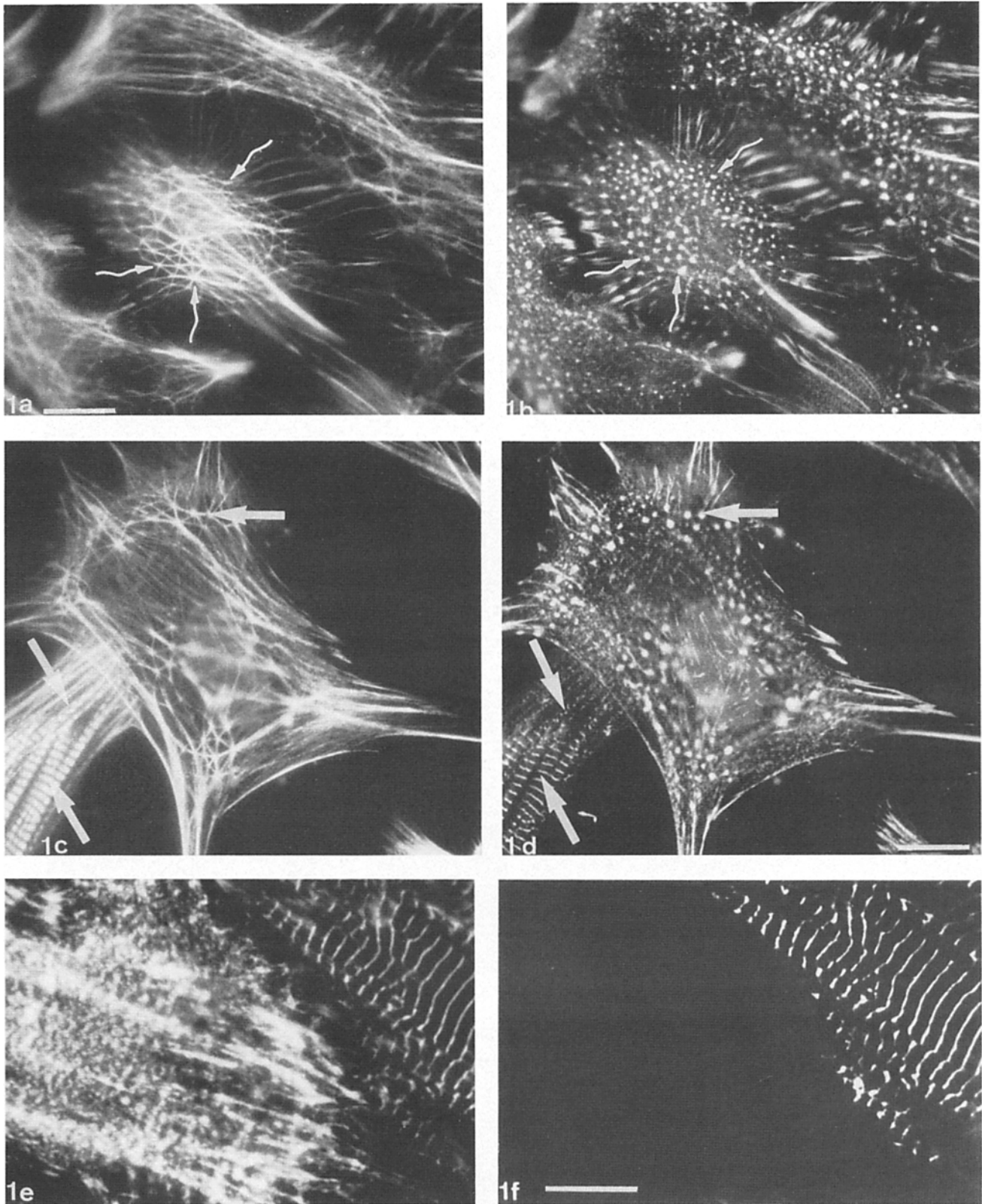
Figure 1. a and b are double-stained fibroblasts from a dense 72-h culture. a shows the distribution of F actin in the fibroblast polygons as revealed by Rho-phalloidin, whereas b reveals the localization of nonmuscle anti–α-actinin (fluorescein channel). Note the colocalization of the two fluorescent reagents at each vertex (*arrows*). c and d are also double-stained with Rho-phalloidin (c) and nonmuscle anti–α-actinin (d; fluorescein channel). The cell in the center is a fibroblast. The lower broad arrows point to the growth tip of a myocyte and its contained nascent nonstriated and striated myofibrils. Note that the F actin struts (a and c) and the α-actinin vertices (b and d) in the fibroblasts polygons vary considerably in size. In contrast, in the myocyte note the constancy in size (1.7–2.0 μm) of the phalloidin stained I–Z–I complexes in c and the constancy in size (0.2 μm) of the Z bands (d). e and f are of a double-stained fibroblast and portion of a myocyte from a day-6 culture, illustrating the differences between the staining properties of the nonmuscle anti–α-actinin and the muscle anti–α-actinin. In addition to staining stress fibers in a punctate fashion, the nonmuscle anti–α-actinin stains Z bands in the myocyte (e; rhodamine channel). The muscle anti–α-actinin only stains the Z bands; it does not stain any structure in the fibroblast. Bars, 10 μm.
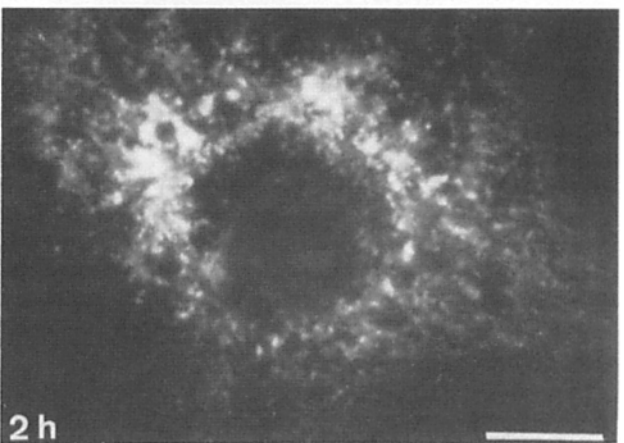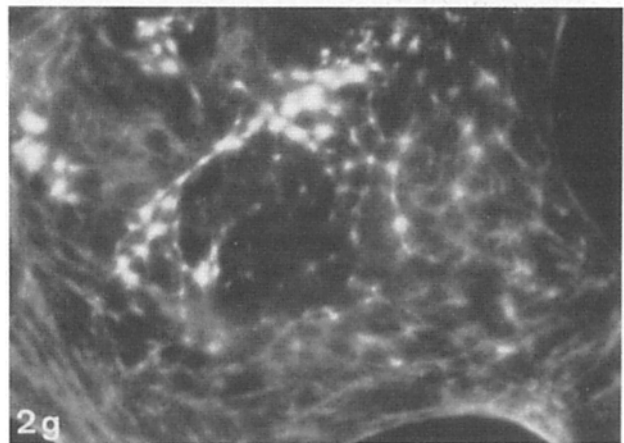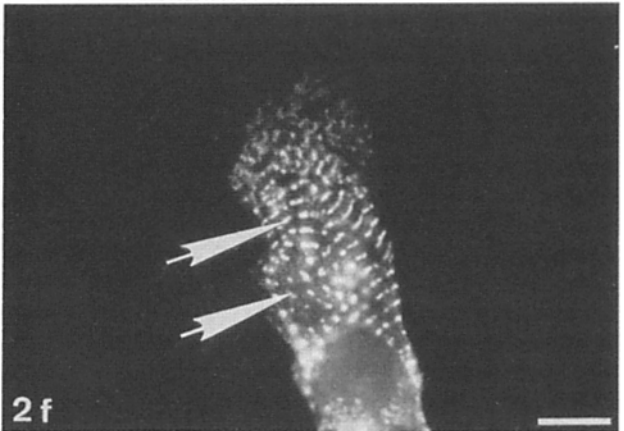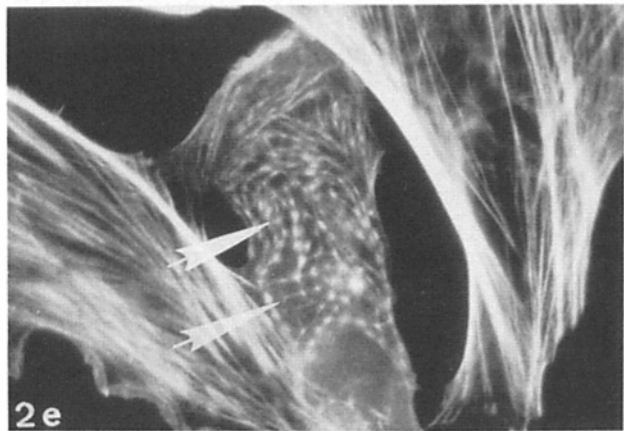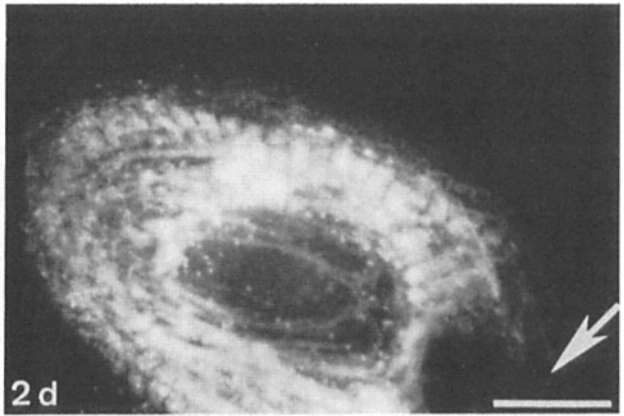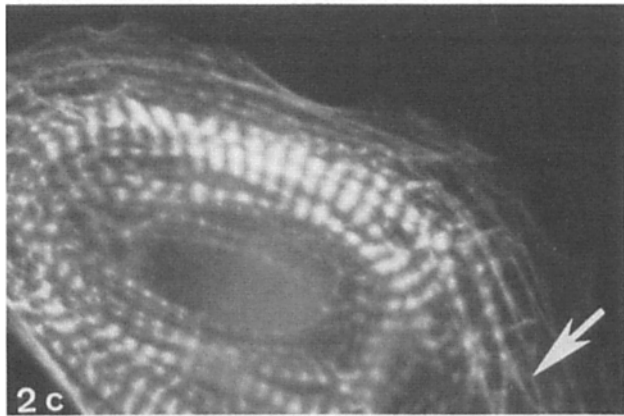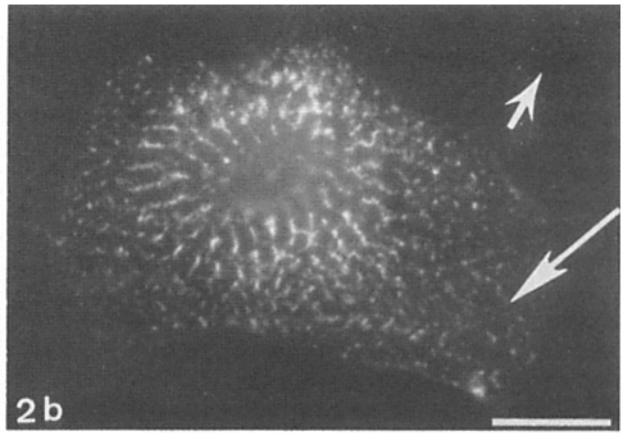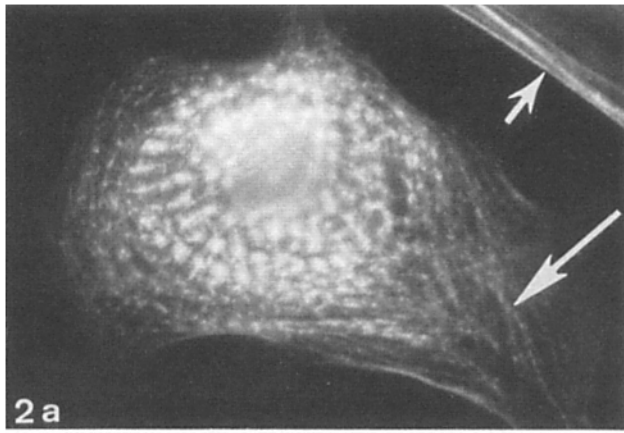
was visualized directly. To stain the same cells with anti-LMM and another rabbit antibody preparation, a previously described (2) procedure was used. After the primary antibody incubation, cells were washed three times, incubated with secondary antibody (labeled goat anti-rabbit IgG; Cooper Biochemical, Malvern, PA), and washed again. Before anti-LMM was applied the cells were incubated for 15-22 min at room temperature in a 1:5 dilution of normal rabbit serum in PBS to saturate exposed goat anti-rabbit IgG sites. Cells were then incubated with anti-LMM, and washed. After staining, cells were mounted by using 60% glycerol with 2.5% DABCO (Sigma Chemical Co., St. Louis, MO) in PBS.

Rhdamine- and FITC-labeled phalloidin, which bind to F-actin, were used to visualize stress fibers and thin filaments within myofibrils. Hoechst dye 33342 was used to stain nuclei. Cells were examined with a Zeiss epifluorescence microscope using excitation filters for either fluorescein or rhodamine fluorescence, and a short-band pass barrier filter for fluorescein which eliminates most bleed-through between channels.

The procedures used for electron microscopy were those described in Antin et al. (2).

Results

Polygonal Networks in Spreading Fibroblasts and Cardiac Myocytes

Roughly half the cells in 36-h cultures are flattened fibroblasts, half still-rounded, minimally attached, contracting myocytes. Fibroblasts are identified as cells displaying numerous parallel stress fibers. These stain uniformly with Rho-phalloidin, but reveal a discontinuous pattern of spacings that vary from 0.6 to 1.2 μm after staining with antibodies to nonmuscle α-actinin and brain MHC (20). Fibroblasts do not stain with antibodies to desmin, muscle MHC, LMM, or muscle α-actinin. Approximately 30% of these cells also exhibit complex polygonal networks. The individual triangles, quadrangles, etc., of this network consist of vertices and connecting struts (Fig. 1, a-d). The vertices, 0.2-2.0 μm in diameter (mean 0.8 μm; $n = 100$) stain with both Rho-phalloidin and nonmuscle anti-α-actinin. The struts vary in length from 1.5 to >6.0 μm (mean 3.5 μm; $n = 100$); they are negative for nonmuscle anti-α-actinin (Fig. 1, b and d), stain uniformly with Rho-phalloidin and discontinuously with antibodies to brain MHC. In spatial arrangements, dimensions and staining properties these geodesic-dome like structures are identical to those described in passaged rat embryonic and 3T3 cells (31, 32, 43).

As stated in Materials and Methods, our rabbit and guinea pig antisera to α-actinin stain dense bodies in stress fibers in fibroblasts, and in addition lightly stain Z bands and their precursor structures in myocytes (Fig. 1, d and e). In contrast, our affinity-purified rabbit antibodies and mAb CP4-10 against muscle α-actinin do not stain any structure in nonmuscle cells (Fig. 1 f and Fig. 2 b and f), but intensely stain Z bands and their precursor structures in both cardiac and skeletal cells (Figs. 1 f, 2 f, 4 a, 6 c). Further work is required to determine whether Z bands and their precursors contain some nonmuscle α-actinin molecules, or whether epitopes detected by nonmuscle anti-α-actinins are also contained in the muscle-specific isoforms.

Cultured myocytes are readily identified as cells binding both myofibril-specific antibodies and antidesmin. The following correlations are based on inspection of many thousands of cultured cells: If a cell binds any one myofibrillar antibody, without exception that cell binds a second. For example, no cell positive for muscle MHC was found to be negative for muscle α-actinin, α-actin, or LMM. Similarly no cell positive for any of the above myofibrillar molecules was found to be negative for desmin. 300 partially rounded myocytes in 36-h cultures were scored for I-Z-I and A band proteins by double-staining with combinations of antibodies to MHC, LMM, muscle α-actinin, α-actin as well as with Rho-phalloidin to detect F actin. Fig. 2, a-h illustrates the variable degree of spreading and different extent of myofibrillar breakdown in these cells. Roughly 25% displayed four or more striated myofibrils, 35% displayed one to three myofibrils, whereas the remaining revealed a variety of double-stained myofibrillar structures in advanced stages of disassembly. Irregular aggregates of MHC-positive material ranging from just resolvable to >3.0 μm in size, are most abundant and characteristic of the 40% of the cells that lacked morphologically distinct striated myofibrils (Fig. 2, g and h). However, as shown in Fig. 2, c and d, even cells with many normal looking myofibrils may display such aggregates. The percentage of cells with MHC aggregates increases between days 2 and 4 in culture and then declines. These MHC aggregates are similar to the MHC-positive debris that emerge after TPA-induced breakdown of myofibrils in cultured skeletal cells (33, 34). The disassembly and degradation of previously functional myofibrils in cultured dissociated cardiac cells obtained from intact embryonic hearts has been described by others (8, 9, 14, 16, 41). Such traumatized myocytes are known to recover, eliminate the myofibrillar debris, and assemble de novo populations of striated, spontaneously contracting myofibrils.

Figure 2. Double-stained individual myocytes from the same 36-h culture. Note the enormous heterogeneity among these cells in terms of overall morphology, degree of spreading, and particularly the number, distribution, and disposition of myofibrillar structures. *a* and *b* illustrate a myocyte stained with Rho-phalloidin (*a*) and muscle anti-α-actinin (*b*; fluorescein channel). Upper arrows point to a nearby fibroblast that is not stained by the muscle anti-α-actinin. The lower arrow points to a region in the spreading lamellapodium where the myofibrils appear to be unraveling into finer filaments. *c* and *d* illustrate a myocyte double-stained with Rho-phalloidin (*c*) and anti-MHC (*d*; fluorescein channel). At this stage many myofibrils still appear reasonably intact after staining with Rho-phalloidin. However, the presence of MHC-patches shown in *d* indicates that considerable breakdown of myofibrils had occurred earlier. To reveal the MHC patches the plane of focus had to be shifted slightly. Arrows in *c* point to a region where myofibrils are unraveling, and concomitantly, where polygons are forming. *e* and *f* illustrate a myocyte and two fibroblasts stained with Rho-phalloidin and muscle anti-α-actinin, respectively. Arrows point to partially contracted and fraying myofibrils and regions of incipient polygon formation. Note total absence of staining by muscle anti-α-actinin of the stress fibers in the two flanking fibroblasts. *g* and *h* are of a myocyte double-stained with Rho-phalloidin and anti-MHC, respectively. All previously assembled striated myofibrils have largely fragmented forming numerous MHC-positive amorphous patches. The brightly staining spots and fine interconnecting filaments in *g* are characteristic of incipient muscle polygons and are analogous to the vertices and struts of polygons in fibroblasts (see below). Bars, 10 μm.
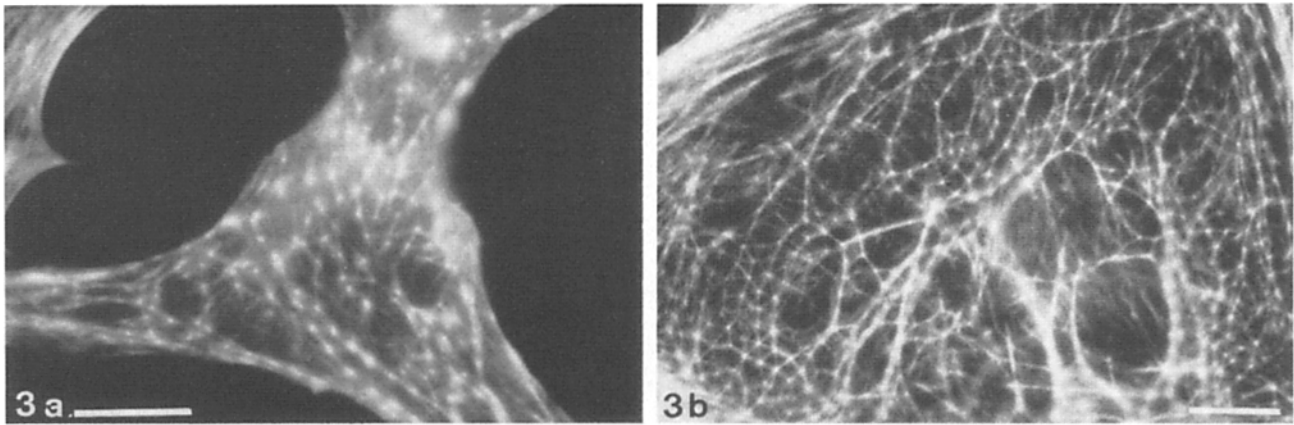
Figure 3. Two Rho-phalloidin stained myocytes from a 48- and 72-h culture. The impression of variably sized struts and vertices in *a* is due to the thickness of the cell and the fact that not all polygons are in the same focal plane. The cell in *b* has spread considerably more and the thickness of the region illustrated is ~0.5 μm, as measured under a confocal microscope. Most of the polygons in *b* are in the same focal plane. Note that the Rho-phalloidin hot spots in both figures are associated with the vertices of the muscle polygons. Often Rho-phalloidin stains nascent Z bands more intensely than the polarized, inserted 1.0-μm-long thin filaments (references 2, 12; see also Figs. 4, *b* and *d*, and 6 *b*). Bars, 10 μm.

Cardiac cells attach and spread more slowly than fibroblasts. Fibroblasts are well-spread by 24 h, whereas many myocytes are still rounded after 48 h. Once lamellapodia form, cardiac cells spread rapidly. Concurrent with spreading are striking changes in the distribution of myofibrillar proteins. Polygons appear in >85% of the myocytes in day 2-3 cultures. These structures costain with Rho-phalloidin and antibodies to muscle α-actinin, MHC, and LMM; they do not stain with anti-brain MHC. Every cell with a muscle polygon also stains with antidesmin, though no obvious morphological connections could be detected with the desmin IFs and the muscle polygons (data not shown). Polygons can be present in cells with what appear to be normal myofibrils as well as in cells that have lost all obvious myofibrils (Figs. 2, *e* and *f* and 3, *a-b*). Polygons increase greatly in number per cell between days 2 and 3 in culture. Figs. 3 *b* and 4, *a-f* illustrate these configurations in detail. Note that striated myofibrils form a continuum with the muscle polygons much as elongated stress fibers merge into polygons in fibroblasts (Fig. 1, *a-d*). Clarity in architectural detail of the muscle polygons varies directly with cell spreading. Measurements of cell thickness with a confocal microscope in steps of 0.3 μm yield values of close to 3.0 μm for a cell similar to that in Fig. 3 *a* to values of 0.3-0.5 μm for cells as flat as those in Figs. 3 *b* and 4, *a-d*. Optical sectioning with the confocal microscope revealed that most of the polygons in Fig. 4, *c* and *d* are contained in a z axis of <0.3 μm.

The vertices of cardiac polygons costain with antibodies to muscle α-actinin and Rho-phalloidin (Fig. 3, *a* and *b* and Fig. 4, *b* and *d*): they are negative for antibodies to both MHC and LMM. The struts of cardiac polygons stain with anti-MHC (Fig. 4, *c* and *e*) and Rho-phalloidin. In spite of over-all similarities in geometry between muscle and fibroblast polygons, it is to be emphasized that the dimensions of the vertices and struts of cardiac polygons are strikingly constant, whereas those of the fibroblasts vary considerably. The mean size for cardiac vertices is 0.2 μm (range 0.2-0.3; n = 100) which contrasts with a mean of 0.8 μm (range 0.2-2.0 μm) for fibroblast vertices. Similarly cardiac struts have a mean of 1.7 μm (range 1.5-1.9; n = 100), whereas fibroblast struts have a mean of 3.5 μm (range 1.5-6.0 μm).

An obvious interpretation of the constancy in size of the vertices and struts of muscle polygons, is that the former represent the 0.2 μm width of early forming Z bands and the latter the 1.7 μm length of newly assembled A bands (1, 2, 11, 22-25, 39, 48). Accordingly, day 4 and 5 cultures were inspected under the electron microscope. Fig. 5, *a* and *b* confirm the notion that myocyte polygons are indeed assembled as multiples of single sarcomeres. Note that each of the sides of the equilateral triangle in Fig. 5 *a* consists of a single, partially contracted sarcomere of interdigitating thick and thin filaments. This is in accordance with the observation that many struts (Fig. 4 *d*) stain throughout with Rho-phalloidin, a condition expected when thin filaments overlap

Figure 4. (*a* and *b*) Double-stained myocytes from a 72-h culture stained with muscle anti-α-actinin to localize Z bands (*a*; fluorescein channel) and Rho-phalloidin to localize F actin in I-Z-I complexes (*b*). Arrows in *a* point to characteristic strings of long, thin myofibrils consisting of 1.7-2.0-μm spacings of α-actinin Z bands. Arrows in *b* point to corresponding I-Z-I complexes stained with Rho-phalloidin. Asterisks mark α-actinin-stained Z bands and their position in the vertices of the corresponding incipient polygon. (*c-f*) A flattened myocyte from a 72-h culture double-stained with anti-MHC (*c*; fluorescein channel) and Rho-phalloidin (*d*). *e* and *f* are tracings of a number of polygons taken from enlarged prints of *c* and *d*. Triangles, circles, and squares mark the corresponding polygons in the four sections. Note that the anti-MHC stains single A bands, leaving the associated I-Z-I complexes unstained. These single A bands constitute the struts of myocyte polygons. The vertices of these triangles, quadrangles, etc., are shown in *d* and *f*. Bars, 10 μm.
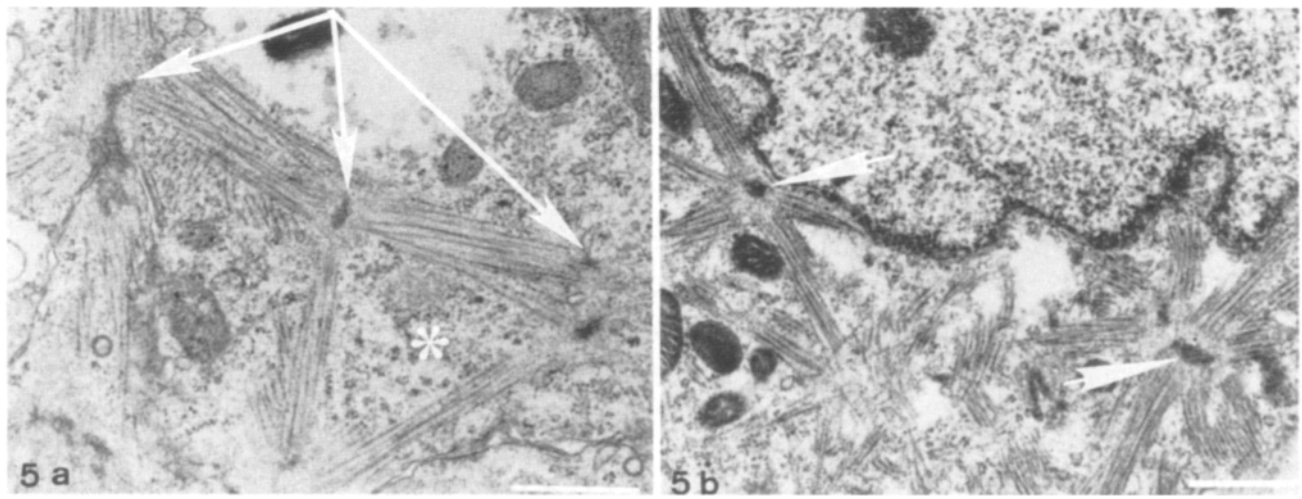
2360
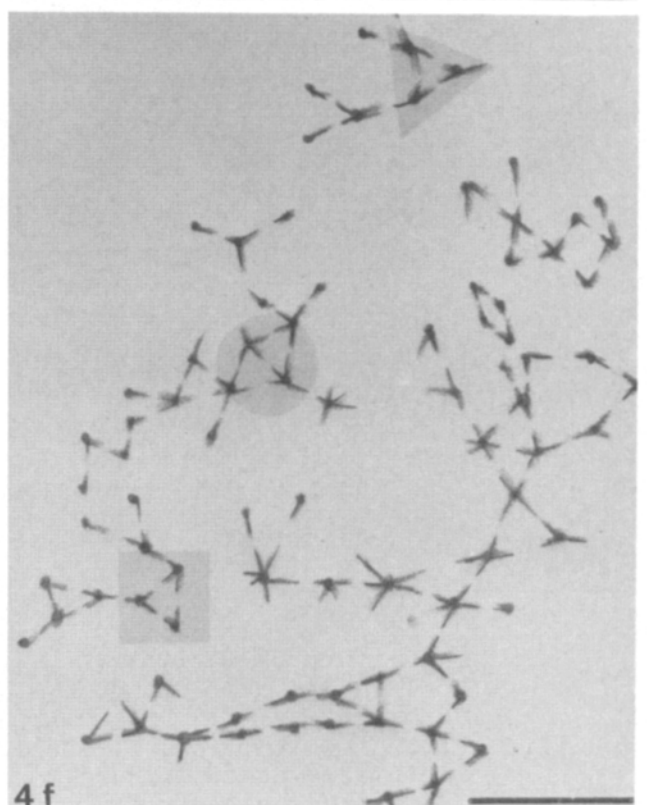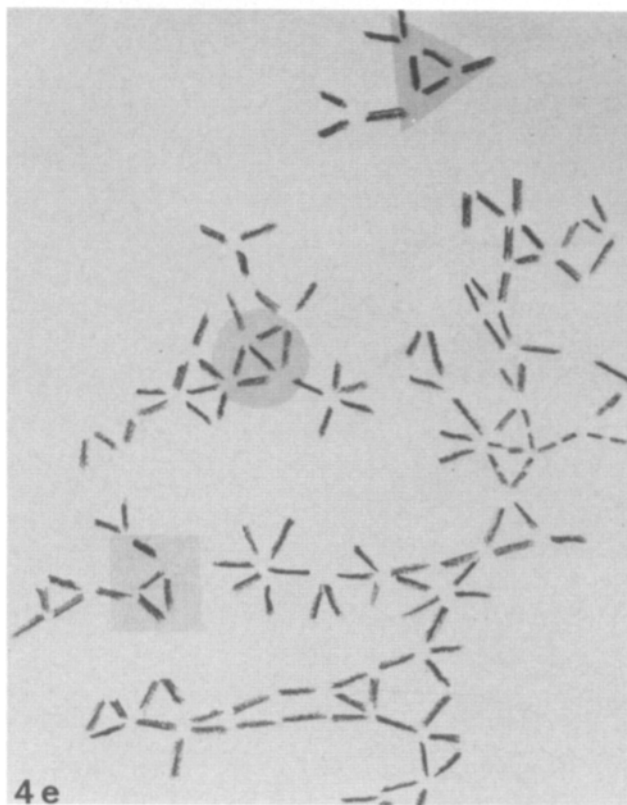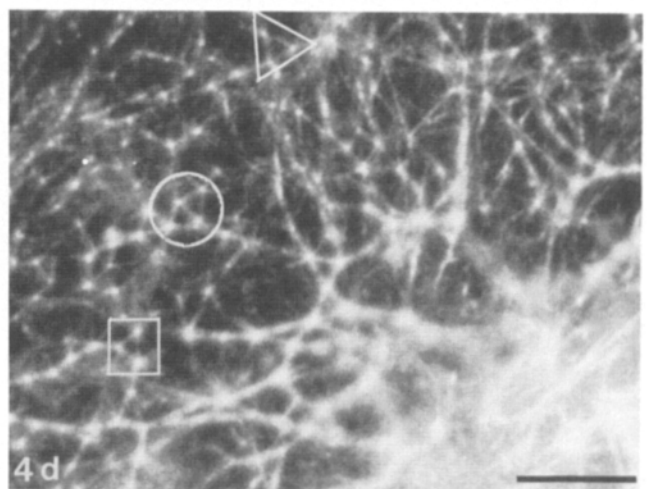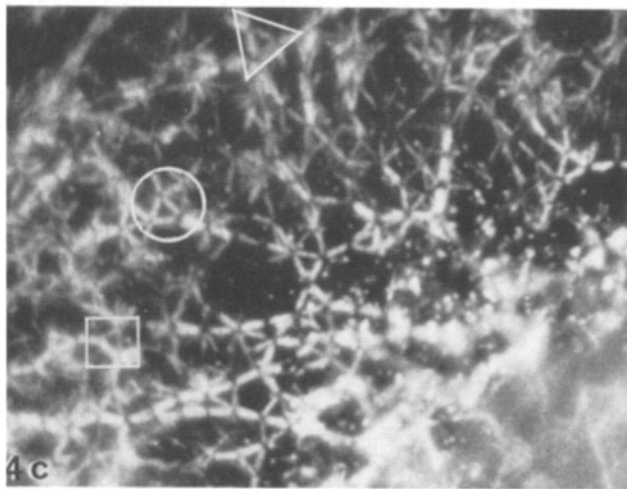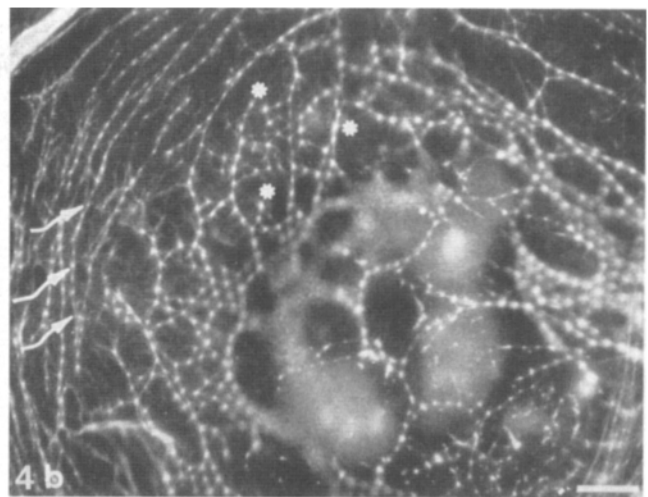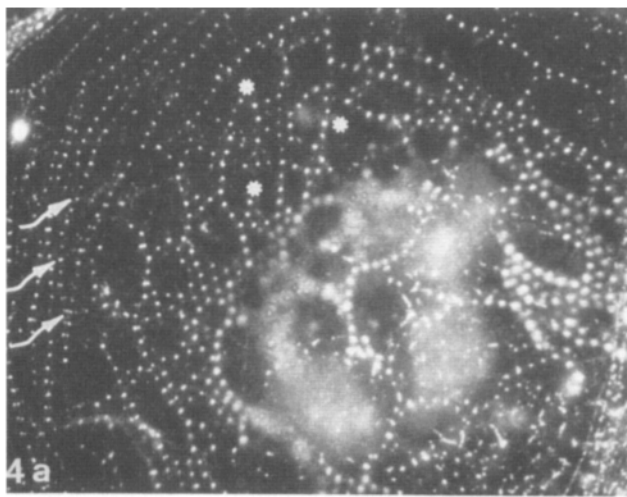
Figure 5. Two electron micrographs of 72-h cultured myocytes. Arrows in *a* point to three consecutive α-actinin Z bands. The irregularly shaped Z band to the left is part of a typical intercalated disc. Choi et al. (7) have shown that such structures are positive for vinculin, muscle α-actinin, and α-actin; in essence these structures are intercellular adhesion plaques. Each side of the equilateral triangle marked by the asterisk consists of a single A band flanked by partially contracted I bands. The vertices of the triangle are irregular Z bands. Arrows in *b* point to two separate I-Z-I complexes that serve as vertices for what in the fluorescence microscope would probably appear as pentagons or hexagons. Bars, 1.0 μm.

in a slightly tilted sarcomere. At higher magnification the centers of several F actin struts (Fig. 4 *f*) display a non-fluorescent gap: these probably represent the H zones or the regions lacking thin filaments in more relaxed sarcomere. Given the thickness of EM sections (roughly 70 nm) and the likelihood of thick and thin filaments and adjacent Z bands going in and out of the plane of section, the correspondence of polygons in the fluorescence and electron micrographs is impressive. These micrographs suggest that the constraints on the respective sizes of the vertices and struts in cardiac polygons reflect the highly ordered packing of the molecules that make up assembled thick and thin filaments and Z bands.

Just as the frequency of geodesic domes diminishes in fully flattened fibroblasts, so their frequency decreases in well-spread myocytes in day 4 and 5 cultures. Cardiac polygons are rarely observed in day 6 and older cultures. When, however, cells from these older cultures are trypsinized and replated as 2° cultures, muscle polygons again appear and again totally disappear after 4–5 d.

Distal Tips of Elongating Myofibrils Terminate in Typical Adhesion Plaques

The termini of elongating stress fibers in many types of non-muscle cells insert into complexes at the cytosolic face of the plasma membrane where the latter adhere to the substrate. These distal tips stain prominently for the cytoskeletal linker proteins talin and vinculin which, along with nonmuscle α-actinin and β- and γ-actin, constitute the characteristic adhesion plaques. It has been suggested that stress fibers elongate centripetally from these adhesion plaques (5, 10, 18, 36, 51). Similarly it has long been proposed (1, 11, 12, 22, 23, 39) that the termini of elongating myofibrils are the site of addition and/or insertion of de novo assembled 1.7 μm sarcomeres.

To determine whether the termini of elongating myofibrils form complexes analogous to those at the ends of stress fibers in nonmuscle cells, day 4–7 cultures were double-stained

with antibodies to vinculin and with either Rho-phalloidin or antibodies to muscle α-actinin or MHC. As documented in Figs. 6, *a–d* and 7, *a–h*, the termini of virtually every nascent myofibril whether striated or nonstriated, display prominent adhesion plaques that stain with antibodies to vinculin and α-actinin, as well as with Rho-phalloidin. The termini of myofibrils are particularly conspicuous where the Rho-phalloidin and muscle anti–α-actinin overlap with the elongated vinculin plaque, a condition often observed at the termini of stress fibers in fibroblasts (Fig. 1, *a–e*). This is of interest, for the tips of stress fibers in fibroblasts involve nonmuscle α-actinin, whereas in the case of myofibrils the analogous structure consists of the muscle α-actinin isoform. Currently we are attempting to determine whether the adhesion plaques of myocytes contain nonmuscle α-actinin in addition to muscle α-actinin. Double-staining experiments with antibodies both to α-actinin and α-actin cannot be performed as the latter requires fixation in methanol which is poor for the former. Separate experiments with mAb to α-actin, however, demonstrate that the F-actin tips of both nascent nonstriated and striated cardiac myofibrils are α-actin positive (see reference 34); it will be of interest to determine whether such sites also contain β- and γ-actins.

Double-staining experiments with antibodies to muscle α-actinin and talin are illustrated in Fig. 6, *e* and *f*. Clearly, in addition to staining the adhesion plaques at the tips of myofibrils, antitalin stains structures in myocytes that are not evident in adjacent fibroblasts. Finding that the adhesion plaques are positive for both vinculin and talin is somewhat unexpected since in mature cardiac cells talin is not present in early intercalated discs where vinculin is found (7, 19).

There are significant differences in the lengths of myofibrils, and hence the distances between their terminal adhesion plaques, in day 3 as compared to day 6 and 7 cultures. As shown in Fig. 7, *a–h*, in early cultures short, individual nascent myofibrils of one to a dozen tandem sarcomeres are common: individual myofibrils with >50 tandem sarcomeres
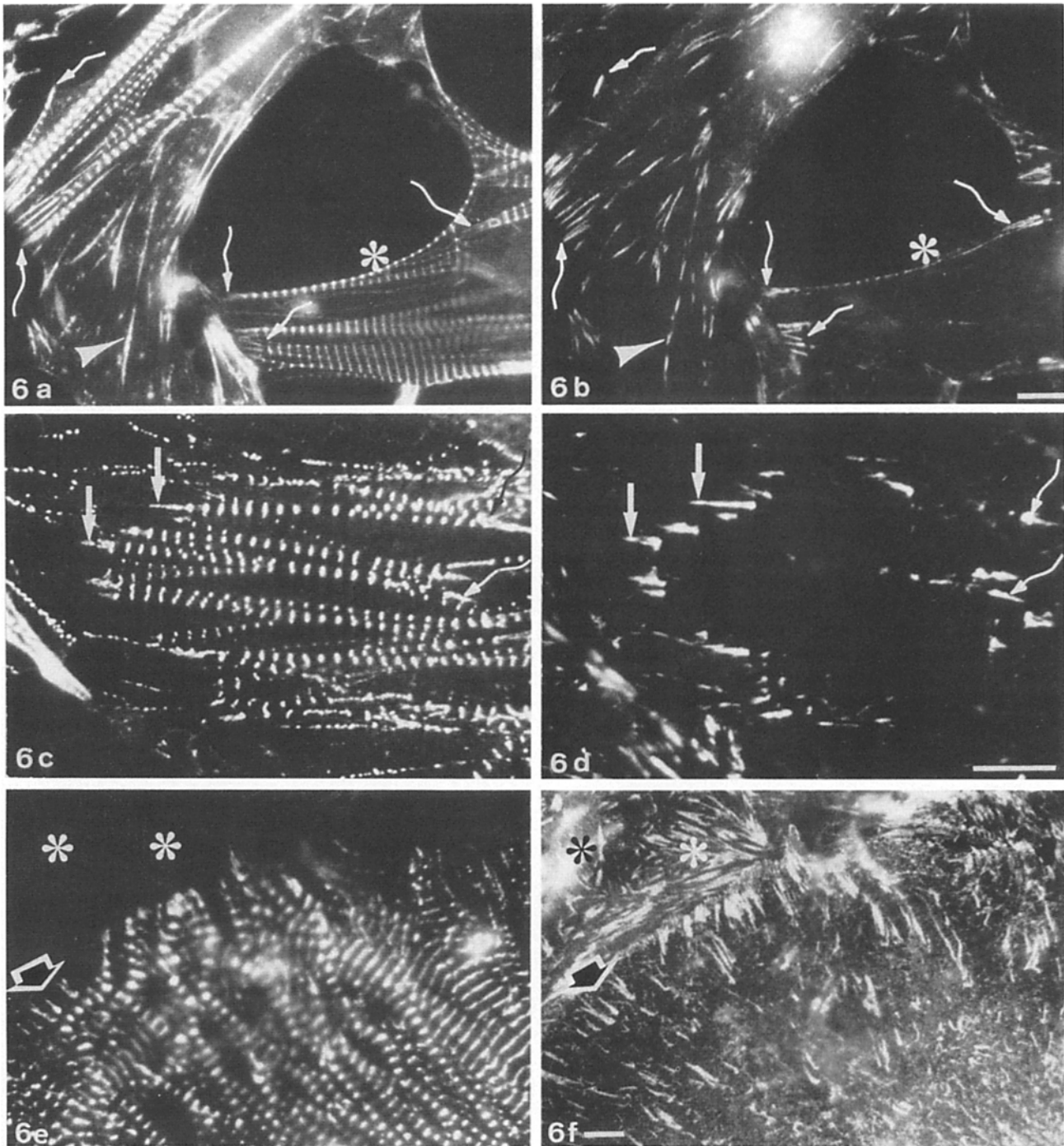
Figure 6. (*a–d*) Double-stained myocytes from a day 6 culture. *a* illustrates the Rho-phalloidin–positive nascent nonstriated and striated myofibrils; *b* illustrates the localization of antivinculin. Observe the intense staining for F actin at the termini of each myofibril and that these tips prominently bind antivinculin (*long curved arrows*). Note also the relatively abrupt transition that proceeds centripetally from the nascent nonstriated myofibril associated with the adhesion plaque, to the striated region of the same myofibril. Asterisk in *b* marks the location of a string of barely resolvable costameres. Arrowheads point to stretches of nascent nonstriated myofibrils, all of which overlap with vinculin. Observe what appears to be largely Z band staining of the relatively mature myofibrils at the lower right of *a*. This is a common condition with Rho-phalloidin staining. The off-rate of Rho-phalloidin binding to the 1.0-μm-long thin filaments in slides stored even for 48 h in the refrigerator, is much greater than at the Z band (unpublished findings). Anomalous staining of myofibrils with Rho-phalloidin associated with contraction has also been reported (2, 12). *c* and *d* are myocytes double-stained with muscle anti α-actinin (*c*); rhodamine channel and antivinculin (*d*; fluorescein channel). Arrows mark the distal tips of the same two striated myofibrils, each consisting of roughly two dozen tandem 1.7–2.0-μm sarcomeres. Again note the abrupt transition from nascent nonstriated to striated region along the same myofibril. (*e* and *f*) A double-stained relatively mature myocyte and two adjacent fibroblasts from a day 7 culture. *e* reveals the localization of muscle anti–α-actinin (rhodamine channel); *f* of antitalin (fluorescein channel). The antitalin stains the termini of most myofibrils, but in addition stains unidentified structures in the myocyte. These additional talin-positive structures are not present in fibroblasts. Bars, 10 μm.
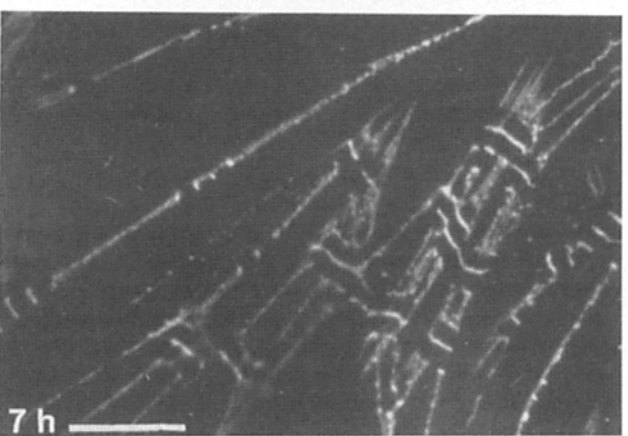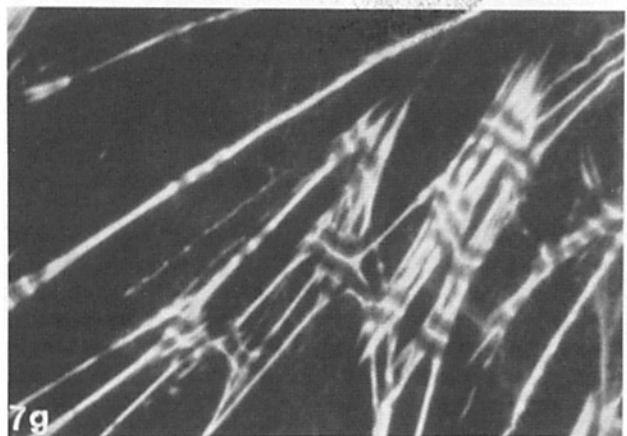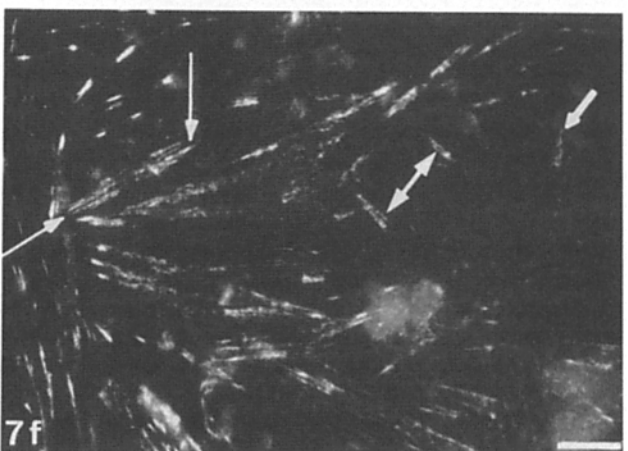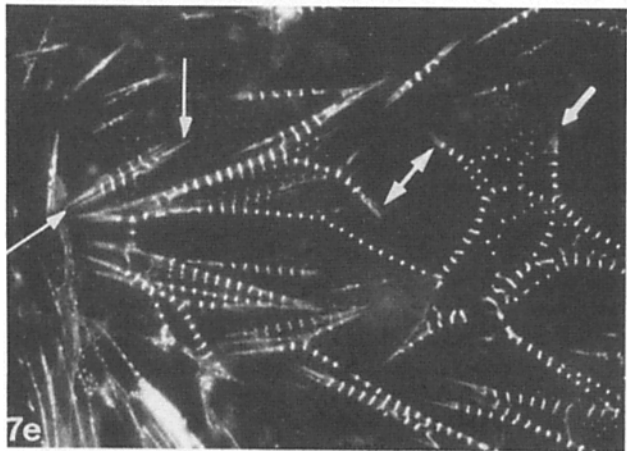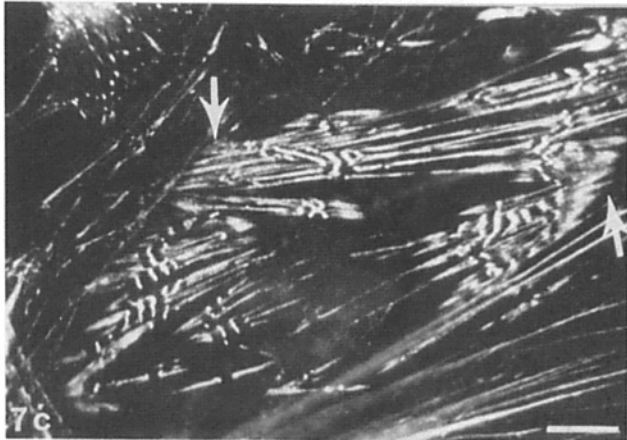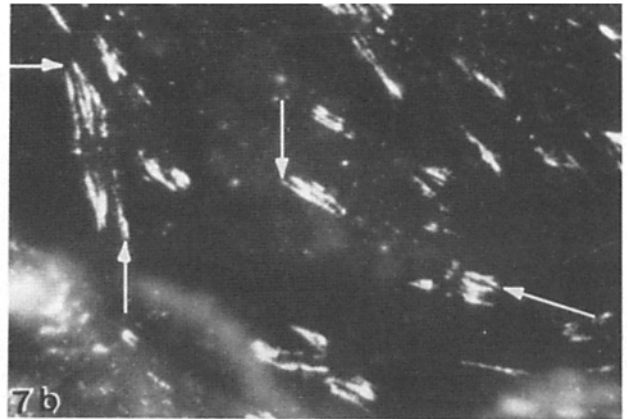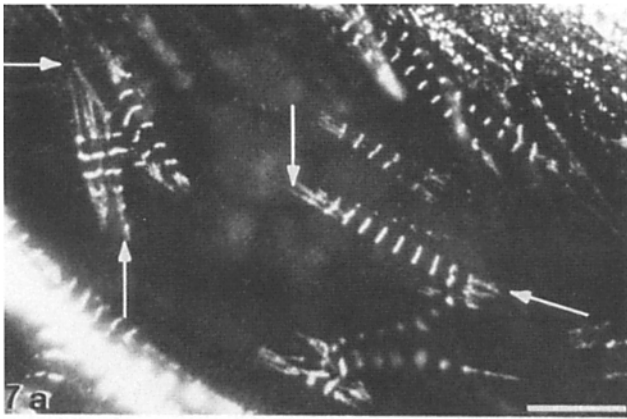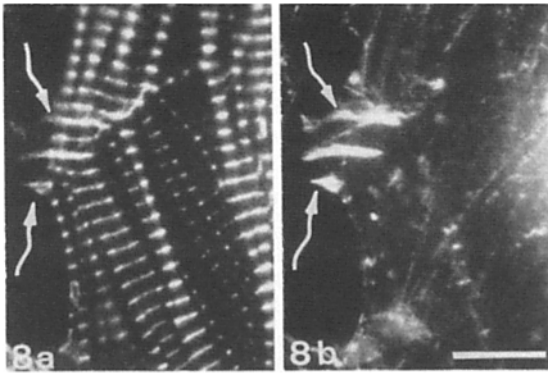
Figure 8. Cultured day 7 myocyte double-stained with muscle anti–α-actinin (*a*; rhodamine channel) and antivinculin (*b*; fluorescein channel). Note that the three prominent vinculin-positive structures stain with muscle anti–α-actinin. The latter structures also merge into Z bands for a number of myofibrils in the upper myocyte. Though not obvious in these micrographs, a diagonally oriented intercalated disk is present at the intersection of the upper and lower cluster of myofibrils. Bar, 10 μm.

are exceptional in these early cultures. The distal tips of short myofibrils stain as brilliantly with Rho-phalloidin and muscle anti–α-actinin as do those of longer myofibrils. Myofibrils of >300 sarcomeres are frequent in day 6 and 7 cultures whereas short myofibrils of less than a dozen sarcomeres are rare. The longitudinal axes of the elongated vinculin plaques parallel those of the inserted myofibrils. Bifurcation of a myofibril distally is accompanied by a bifurcation of the vinculin plaque. The adhesion plaque complex at the ends of each myofibril often consists of multiple strands (Fig. 7, *a–h*). Most intriguing, however, is the observation that during the entire period of elongation when myofibrils with few sarcomeres are elongating into myofibrils with many sarcomeres, the talin/vinculin plaques appear to maintain their physical continuity with the respective ends of each myofibril. Somehow as a short myofibril elongates by the addition distally of single 1.7–2.0-μm sarcomeres, there must be a corresponding distal displacement of the two terminal adhesion plaques at the ends of that myofibril (see Discussion).

There are other changes in early vs. older cultures regarding the distribution of adhesion plaques. In early cultures plaques of various lengths are observed intermittently along the length of immature myofibrils of <20–30 tandem sarcomeres (Figs. 6 *a* and 7, *e* and *f*). These must be transitory

structures, since they disappear in virtually all myocytes with more mature myofibrils of 50 or more tandem sarcomeres present in day 5 and older cultures. This loss of plaques along the length of myofibrils most probably correlates with the displacement of myofibrils from their original submembraneous location (2, 12, 33). The consequence of these changes in distribution of adhesion plaques is that in day 6 and 7 cultures all α-actinin/vinculin complexes are confined to the ends of long myofibrils, where they associate with the sarcolemma. This may be either at a free border or at the sites of juxtaposed cell membranes where the cells assemble typical, if spatially distorted intercalcated disks (Fig. 8). A small number of myofibrils bind antivinculin (Fig. 6 *b*) to costamere-like structures (40). The significance of this staining, and why only a subset of Z band–like structures stains is unknown.

These experiments involving the termini of elongating myofibrils also are of interest for demonstrating the equivalent behavior of the α-actinin isoforms. Images such as those in Fig. 8, *a* and *b* suggest that the same local aggregation of muscle α-actinin molecules which participates in the assembly of a given Z band also participates in the assembly of a typical adhesion plaque. Such chimeric structures (part Z band, part adhesion plaque) mimics the in vivo arrangement of the same isoforms that occurs periodically along the intercalated disk. The intermittent fasciae adherentes that constitute the intercalated disk consist of a meshwork of muscle α-actinin which complexes distally with vinculin and proximally with the barbed ends of 1.0-μm-long α-actin filaments (7, 19, 21, 49–51). More recently Schultheiss and Holtzer (unpublished data) have found that the step-like regions between two cardiac cells indicated in Fig. 8 also bind antibodies against the desmoplakins and cytokeratins; molecules normally associated with the desmosomes that form part of the intercalated disk (7).

Discussion

The static micrographs that form the basis of this report do not immediately lend themselves to a mechanistic explanation of the causes of the disassembly of functional myofibrils and the formation of transitory cardiac polygons in dissociated myocytes. Similarly, noting that every nascent myofibril of 0, 1, 20, 60, . . . *n* sarcomeres is capped at both ends by adhesion plaques does not immediately suggest how intact 1.7–2.0-μm sarcomeres might insert at the distal tips of elongating myofibrils. However, the description of these

---

Figure 7. Double-stained myocytes from day 5 cultures that illustrate the tight linkage between the termini of each myofibril and the vinculin-positive adhesion plaques. *a* and *b* are stained with muscle anti–α-actinin (*a*, fluorescein channel) and antivinculin (*b*; rhodamine channel). Arrows point to two nascent myofibrils of 4–5 and 10 sarcomeres, respectively. These two nascent myofibrils display unusually modest nonstriated ends. *c* and *d* are also double-stained with muscle anti–α-actinin and antivinculin to illustrate another common arrangement of nascent nonstriated and striated myofibrils and their terminal vinculin-positive adhesion plaques. Arrows point to the termini of parallel clusters of elongating myofibrils. Note that though the nonstriated condition is most common at the distal tips of myofibrils, not infrequently regions in the middle of a given myofibril also appear to be nonstriated (see references 12, 22). *e* and *f* are double-stained with Rho-phalloidin and antivinculin (*f*; fluorescein channel). The spots in *f* are due to bleed-through from Hoechst stained nuclei. Note that the longitudinal axis of each adhesion plaque reflects the local axis of the immediately adjoining part of the myofibril. *g* and *h* are high magnifications of a region double-stained with Rho-phalloidin (*g*) and muscle anti–α-actinin (*h*; fluorescein channel). Note both long and short stretches of nonstriated myofibrils and the fact that the termini of each myofibril, as the termini of each stress fiber, stain prominently for F-actin and α-actinin. Bars, 10 μm.

unexpected juxtapositions of myofibrillar and cytoskeletal molecules encourages experiments that otherwise might not have been considered. At a minimum they draw attention to the fact that whereas there is a modest knowledge of the genetic mechanisms that up- and down-regulate the synthesis of myofibrillar proteins, virtually nothing is known of those mechanisms which order the newly synthesized proteins into tandem sarcomeres or those responsible for maintaining their morphological and functional integrity.

Studies detailing the distribution of β- and γ-actins and of nonmuscle α-actinin in stress fibers have been made largely on flattened nontranslocating, nonmuscle cells. In rounded and motile cells (and in viral infected cells) these proteins are thought to be in soluble pools (31, 43, 45). Nothing is known of the intracellular conditions that induce the formation of polygons in either fibroblasts or myocytes as opposed to the assembly of longitudinally oriented stress fibers and/or myofibrils. Though polygons are most conspicuous when rounded fibroblasts flatten, whether they are also induced when flattened cells round up has yet to be demonstrated. In the former instance, presumably the soluble isoforms polymerize into polygons of different sized vertices and struts. If polygons also appear in the latter case, then a form of splitting and reorganization of already-assembled stress fibers may be involved. The data in this report do not rule out the possibility that soluble muscle isoforms directly polymerize into polygons, for branched myofibrils are common in normal developing heart cells (16, 21). However, the notion of splitting of preexisting myofibrils is favored for a number of reasons. Every plated cardiac cell originally contained many striated myofibrils (7, 8, 9, 12, 16, 41). Over 85% of the myocytes in day 2 and 3 cultures display polygons and most such cells also display MHC patches, a sensitive indicator of earlier myofibrillar breakdown (34, 35). Virtually all cardiac polygons have disappeared in day 5 cultures. Together these findings suggest that muscle polygons represent an unexpected transient phase in the fragmentation and elimination of previously assembled and functional myofibrils. If this interpretation is correct, polygons are probably unstable structures and play no significant role in the assembly of myofibrils. They may, however, be pertinent to the way in which injured cardiac cells clear damaged myofibrils. It will be interesting to learn if the breakdown of muscle polygons enriches the soluble pool of muscle isoforms, or, as has been suggested for TPA-induced breakdown of myofibrils (34, 35), whether such proteins are not reused, but are packaged and directly eliminated from the cell.

Complexes of vinculin/nonmuscle α-actinin/β- and γ-actin link stress fibers to the cytoplasmic face of the cell membrane at all adherens junctions. Their presence in intestinal, liver, and smooth muscle cells, as well as in cultured fibroblasts and cardiac cells suggests the three proteins have been selected to colocalize at the cell surface and interact with one another irrespective of neighboring membrane cell-specific molecules (49–51). The substitution of muscle α-actinin for the nonmuscle isoform in the adhesion plaques of myocytes testifies to common properties of the two isoforms. In the hybrid complex illustrated in Fig. 8, muscle α-actinin interacts with the barbed ends of α-actin myofilaments at one site and with vinculin at another, much as nonmuscle α-actinin in stress fibers interacts with β- and γ-actins at one site and with vinculin at another.

There are differences in opinion as to the precise spatial and temporal distribution of vinculin, F actin, and α-actinin in the formation of adhesion plaques in fibroblasts (10, 18). Nevertheless, all investigators concur in the observation that in fibroblasts the merging of a nascent vinculin plaque with a "precursor stress fiber structure" consisting of α-actinin and F actin stabilizes both structures. Of even greater interest, the photobleaching experiments of Kreis et al. (29), Wang (53), and McKenna et al. (36) suggest that these complexes play major roles in the initiation of the assembly of stress fibers and in the ensuring of their appropriate centripetal growth in nonmuscle cells. The presence of the vinculin/muscle α-actinin/α-actin complexes at both ends of all myofibrils, irrespective of size or orientation, is consistent with the idea that such complexes play an analogous role for myofibrils. The data in this report are consistent with the notion that the adhesion plaque/SFLS complex is a dynamic site which determines not only the primary site of nucleation of each future striated myofibril, but also determines the future trajectory of each nascent myofibril (Fig. 7, a–h).

The notion that a single myofibril may elongate from one to several hundred tandem sarcomeres while remaining attached to its two oppositely located adhesion plaques is not easy to visualize. Nevertheless Figs. 6 and 7 require that this notion be seriously considered. The insertion of a unit 1.7–2.0-μm sarcomere between a submembraneous adhesion plaque and the terminal 0.2-μm-wide muscle α-actinin Z band of an elongating myofibril must involve multiple levels of macromolecular organization still poorly understood. Sarcomeres are intrinsically bipolar structures; there is a twofold symmetry axis through both the M line and Z line (26). The addition of a sarcomeric unit at the ends of myofibrils probably involves mechanisms somewhat different from the addition of β- and γ-actin monomers at the termini (a) of elongating stress fibers in nonmuscle cells, (b) of elongating acrosomes (47), and (c) of elongating thin filaments in brush borders of intestinal epithelial cells (37). Nevertheless in all these systems the addition of new molecules responsible for elongation occurs at a submembraneous site.

Sanger and co-workers (38, 44, 44a) have proposed that the transition from nascent nonstriated to striated myofibril involves precursor strings of "mini-sarcomeres." We find no evidence that closely spaced Z bands, including short thick filaments, monotonically lengthen until they achieve the dimensions of definitive sarcomeres. We are impressed with how sharply the most distal Z band of the terminal 1.7-μm sarcomere marks the boundary between striated and nonstriated domains of a given myofibril.

The findings in this study regarding the intimate relationship between the cytoskeletal structures lining the inner surface of the myocyte membrane and the "birth-site" of the nascent myofibril confirm and extend the recent observations of Choi et al. (7). These investigators studied the intact hearts of 40–50-h embryos, the time when the primitive heart initiates spontaneous contractions. They concluded that (a) the first nascent myofibril with a 1.7–2.0-μm sarcomeric periodicity forms a circumferential ring analogous to the terminal web in other types of epithelial cells; and (b) the tips of each nascent myofibril inserts into an intercalated disk that consists of a vinculin/muscle α-actinin/α-actin complex. Clearly the elongated vinculin/muscle α-actinin/α-actin complexes documented in Figs. 6, 7, and 8 are the functional, though spatially distorted, equivalents of in vivo intercalated disks. In brief, though there are programmed differences regarding

which cohort of myofibrillar genes will be active in 40–50 h, vs. 7–10-d cardiac myocytes, the rules governing the assembly of thick and thin filaments and Z bands into tandem sarcomeres are fundamentally the same at both stages of development as well as in vivo and in vitro.

References

1. Antin, P., S. Forry-Schaudies, T. Friedman, S. Tapscott, and H. Holtzer. 1981. Taxol induces postmitotic myoblasts to assemble interdigitating microtubule-myosin arrays that exclude actin filaments. *J. Cell Biol.* 90:300–308.
2. Antin, P., S. Tokunaka, V. Nachmias, and H. Holtzer. 1986. Role of stress fiber-like structures in assembling nascent myofibrils in recovering ethyl methanesulfonate myosheets. *J. Cell Biol.* 102:1464–1479.
3. Atherton, B., D. Meyer, and D. Simpson. 1986. Assembly and remodeling of myofibrils and intercalated discs in cultured neonatal rat heart cells. *J. Cell Sci.* 86:233–248.
4. Bennett, G., S. Fellini, Y. Toyama, and H. Holtzer. 1979. Redistribution of intermediate filament subunits during skeletal myogenesis and maturation in vitro. *J. Cell Biol.* 82:577–584.
5. Burridge, K. 1986. Substrate adhesions in normal and transformed fibroblasts. Organization and regulation of cytoskeletal, membrane and extracellular matrix components at focal contacts. *Cancer Rev.* 10:18–78.
6. Burridge, K., and L. Connell. 1983. Talin: a cytoskeletal component concentrated in adhesion plaques and other sites of actin membrane interaction. *Cell Motil.* 3:405–417.
7. Choi, J., T. Schultheiss, M. Lu, W. Franke, D. Bader, D. Fischman, and H. Holtzer. 1988. Founder cells for the cardiac and skeletal myogenic lineages. *In* Cellular and Molecular Biology of Muscle Development. F. Stockdale and L. Kedes, editors. Alan R. Liss, Inc. NY. 27–36.
8. Claycomb, W. C., and H. D. Bradshaw, Jr. 1983. Acquisition of multiple nuclei and the activity of DNA polymerase a and reinitiation of DNA replication in terminally differentiated adult cardiac muscle cells in culture. *Dev. Biol.* 99:331–337.
9. Dehaan, R. L. 1967. Regulation of spontaneous activity and growth of embryonic chick heart cells in tissue culture. *Dev. Biol.* 16:216–249.
10. Depasquale, J. A., and D. S. Izzard. 1987. Evidence for an actin-containing cytoplasmic precursor of the focal contact and the timing of incorporation of vinculin at the focal contact. *J. Cell. Biol.* 105:2803–2809.
11. Dienstman, S., and H. Holtzer. 1975. Myogenesis: a cell lineage interpretation. *Results Probl. Cell Differ.* 7:1–25.
12. Dlugosz, A., P. Antin, V. Nachmias, and H. Holtzer. 1984. The relationship between stress fiber-like structures and nascent myofibrils in cultured cardiac myocytes. *J. Cell. Biol.* 99:2268–2278.
13. Emerson, C., D. Fischman, B. Nadal-Ginard, and M. Siddiqui. 1985. Molecular Biology of Muscle Development. Alan R. Liss, Inc., NY. 953 pp.
14. Eppenberger, M., I. Hauser, T. Baechi, U. Brunner, C. Dechesne, and H. Eppenberger. 1988. Immunocytochemical analysis of the regeneration of myofibrils in long-term cultures of adult cardiomyocytes of the rat. *Dev. Biol.* 130:1–15.
15. Endo, T., and T. Masaki. 1984. Differential expression and distribution of chicken skeletal- and smooth-muscle type α-actinins during myogenesis in culture. *J. Cell Biol.* 99:2322–2335.
16. Etlinger, J., and D. Fischman. 1973. M and Z band components and the assembly of myofibrils. *Cold Spring Harbor Symp. Quant. Biol.* 37:511–522.
17. Fischman, D. 1986. Myofibrillogenesis and the morphogenesis of skeletal muscle. *In* Myology. A. Engle and B. Banker, editors. McGraw-Hill Inc., New York. 5–37.
18. Geiger, B., Z. Avnur, T. Kreis, and J. Schlessinger. 1984. The dynamics of cytoskeletal organization in areas of cell contact. *Cell Muscle Motil.* 5:195–234.
19. Geiger, B., T. Volk, and T. Volberg. 1985. Molecular heterogeneity of adherens junctions. *J. Cell Biol.* 101:1523–1531.
20. Gordon, W. E. 1978. Immunofluorescent and ultrastructural studies of "sarcomeric" units in stress fibers of cultured non-muscle cells. *Exp. Cell Res.* 117:253–260.
21. Hagopian, M., and D. Spiro. 1970. Derivation of the Z line in the embyronic chick heart. *J. Cell Biol.* 44:683–687.
22. Hill, C., S. Duran, Z. Lin, K. Weber, and H. Holtzer. 1986. Titin and myosin, but not desmin are linked during myofibrillogenesis in postmitotic mononucleated myoblasts. *J. Cell Biol.* 103:2185–2196.
23. Holtzer, H., J. Marshall, and H. Finck. 1957. An analysis of myogenesis by use of fluorescent antimyosin. *J. Biophys. Biochem. Cytol.* 3:705–725.

24. Holtzer, H., J. Sanger, H. Ishikawa, and K. Strahs. 1973. Selected topics in skeletal myogenesis. *Cold Spring Harbor Symp. Quant. Biol.* 37:549–566.
25. Holtzer, H., J. Sasse, A. Horwitz, P. Antin, and M. Pacifici. 1986. Myogenic lineages and myofibrillogenesis. *Bibl. Anat.* 29:109–125.
26. Huxley, H. 1983. Molecular basis of contraction in cross-striated muscles and relevance to motile mechanisms in other cells. *In* Muscle and Non-Muscle Motility. A. Stracher, editor. Academic Press Inc., New York. 1–104.
27. Ishikawa, H., R. Bischoff, and H. Holtzer. 1968. Mitosis and intermediate-sized filaments in developing skeletal muscle. *J. Cell Biol.* 38:538–555.
28. Ishikawa, H., R. Bischoff, and H. Holtzer. 1969. Formation of arrowhead complexes with heavy meromyosin in a variety of cell types. *J. Cell Biol.* 43:312–332.
29. Kreis, T., B. Geiger, and J. Schlessinger. 1982. Mobility of microinjected rhodamine actin within living chicken gizzard cells determined by fluorescence photobleaching recovery. *Cell.* 29:835–845.
30. Langanger, G., M. Moeremans, G. Daniels, M. DeBrander, and J. DeMay. 1986. The molecular organization of myosin in stress fibers of cultured cells. *J. Cell Biol.* 102:200–209.
31. Lazarides, E., and K. Burridge. 1975. α-Actinin: immunofluorescent localization of a muscle structural protein in non-muscle cells. *Cell.* 6:289–298.
32. Lazarides, E. 1976. Actin, α-actinin, and tropomyosin interaction in the structural organization of actin filaments in nonmuscle cells. *J. Cell Biol.* 68:202–219.
33. Legato, J. 1972. Ultrastructural characteristics of the rat ventricular cell grown in tissue-culture with special reference to sarcomerogenesis. *J. Mol. Cell Cardiol.* 4:209–317.
34. Lin, Z., J. Eshleman, S. Forry-Schandies, S. Duran, J. Lessard, and H. Holtzer. 1987. Sequential disassembly of myofibrils induced by phorbol myristate acetate in cultured myotubes. *J. Cell Biol.* 105:1365–1376.
35. Lin, Z., J. Eshleman, C. Grund, D. Fischman, T. Masaki, W. Franke, and H. Holtzer. 1989. Differential response of myofibrillar and cytoskeletal proteins in cells treated with phorbol myristate acetate. *J. Cell Biol.* 108:1079–1091.
36. McKenna, N., C. Johnson, and Y. Wang. 1986. Formation and alignment of Z lines in living chick myotubes microinjected with rhodamine-labelled alpha-actinin. *J. Cell Biol.* 103:2163–2171.
37. Mooseker, M., and L. Tilney. 1975. Organization of an actin filament-membrane complex, filament polarity, and membrane attachment in the microvilli of intestinal epithelial cells. *J. Cell Biol.* 67:725–743.
38. Mittal, B., J. Sanger, and J. Sanger. 1987. Visualization of myosin in living cells. *J. Cell Biol.* 105:1753–1760.
39. Okazaki, K., and H. Holtzer. 1965. An analysis of myogenesis in vitro using fluorescein-labelled antimyosin. *J. Cytol. Histochem.* 13:726–739.
40. Pardo, J., J. D'Angelo, and S. Craig. 1983. Vinculin is a component of an extensive network of myofibril-sarcolemma attachment regions in cardiac muscle fibers. *J. Cell Biol.* 97:1081–1088.
41. Perissel, B., J. Charbronne, M. Moalic, and P. Malet. 1980. Initial stages of trypsininzed cell culture of cardiac myoblasts. *J. Mol. Cell. Cardiol.* 12:63–75.
42. Pette, D. 1980. Plasticity of Muscle. Walter de Gruyter & Co., Berlin/New York. 146 pp.
43. Rathke, P. C., M. Osborn, and K. Weber. 1979. Immunological and ultrastructural characterization of microfilaments bundles; polygonal nets and stress fibers in an established cell line. *Eur. J. Cell Biol.* 19:40–48.
44. Sanger, J., B. Mittal, M. Pochapin, and J. Sanger. 1986. Myofibrillogenesis in living cells microinjected with fluorescently labeled alpha-actinin. *J. Cell Biol.* 102:2053–2066.
44a. Sanger, J., B. Mittal, T. Meyer, and J. Sanger. 1989. Use of fluorescent probes to study myofibrillogenesis. *In* Cellular and Molecular Biology of Muscle Development. F. Stockdale and L. Kedes, editors. Alan R. Liss, Inc., New York. 221–236.
45. Shriver, K., and L. Rohrschneider. 1981. Organization of pp60src and selected cytoskeletal proteins within adhesion plaques and junctions of Rous sarcoma virus-transformed rat cells. *J. Cell Biol.* 89:525–535.
46. Stockdale, F., and L. Kedes. 1988. Cellular and molecular biology of muscle development. *UCLA (Univ. Calif. Los Angel.) Symp. Mol. Cell. Biol. New Ser.* 93:1–1059.
47. Tilney, L., E. Bonder, and D. DeRosier. 1981. Actin filaments elongate from their membrane-associated ends. *J. Cell Biol.* 90:485–494.
48. Toyama, Y., B. S. Forry-Schandies, B. Hoffman, H. Holtzer. 1982. Effect of taxol and colcemid on myofibrillogensis. *Proc. Natl. Acad. Sci. USA.* 79:6556–6566.
49. Tsukita, S., and S. Tsukita. 1989. Isolation of cell-to-cell junctions from rat liver. *J. Cell Biol.* 108:31–41.
50. Volberg, T., B. Geiger, J. Kartenbeck, and W. Franke. 1986. Changes in membrane-microfilament interaction in intercellular adherens junctions upon removal of extracellular CA ions. *J. Cell Biol.* 102:1832–1842.
51. Volk, T., and B. Geiger. 1986. A-CAM: 135-kD receptor of intercellular adherens junctions. I. Immunoelectron microscopic localization and biochemical studies. *J. Cell Biol.* 103:1451–1460.
52. Wang, S., M. Greaser, E. Schults, J. Bulinski, J. Lin, and J. Lessard. 1988. Studies on cardiac myofibrillogenesis with antibodies to titin, actin, tropomyosin and myosin. *J. Cell Biol.* 107:1075–1083.
53. Wang, Y. 1985. Exchange of actin subunits at the leading edge of living fibroblasts: possible role of treadmilling. *J. Cell Biol.* 101:597–602.